



HAL
open science

Optical bacteriophage susceptibility testing by SPR (surface plasmon resonance)

Larry Kingston-O'Connell, Yoann Roupioz, Pierre Marcoux

► **To cite this version:**

Larry Kingston-O'Connell, Yoann Roupioz, Pierre Marcoux. Optical bacteriophage susceptibility testing by SPR (surface plasmon resonance). Proceedings Volume 11661, Plasmonics in Biology and Medicine XVIII, Mar 2021, Californie (Online Only), United States. pp.15, 10.1117/12.2578753 . hal-03408415

HAL Id: hal-03408415

<https://hal.science/hal-03408415>

Submitted on 3 Nov 2021

HAL is a multi-disciplinary open access archive for the deposit and dissemination of scientific research documents, whether they are published or not. The documents may come from teaching and research institutions in France or abroad, or from public or private research centers.

L'archive ouverte pluridisciplinaire **HAL**, est destinée au dépôt et à la diffusion de documents scientifiques de niveau recherche, publiés ou non, émanant des établissements d'enseignement et de recherche français ou étrangers, des laboratoires publics ou privés.

Optical Bacteriophage Susceptibility Testing by SPR (Surface Plasmon Resonance)

Larry O'Connell ^{a,b}, Yoann Roupioz ^b, Pierre Marcoux ^a.

^aUniv. Grenoble Alpes, CEA, LETI, F38054 Grenoble, France; ^bUniv. Grenoble Alpes, CNRS, CEA, IRIG, SyMMES, 38000 Grenoble, France.

ABSTRACT

The proliferation of multiresistant bacteria is having an increasing and profound impact on the world. A credible alternative to antibiotics is bacteriophage therapy, which are expected in the near future to form the basis of an entirely new treatment paradigm for infectious diseases. In order to facilitate such an epochal transition, new tools are needed for the rapid and multiplexed screening of large libraries of candidate bacteriophages in order to provide a personalized bacteriophage cocktail for each patient. This talk presents recent progress towards the development of a SPR-based screening method, wherein immobilized bacteriophages form a biosensing layer which produces a measurable surface plasmon resonance signal as a result of the specific interaction between the bacteriophages and their host bacterial cells in a microfluidic flow above the sensor surface.

Keywords: Biomaterials, Biosensing, Functional surfaces, Surface functionalization, Bacteriophage, Surface Plasmon Resonance

1. INTRODUCTION

The ability to overcome common infections and enjoy the benefits of routine surgery has come to characterize contemporary life at such a profound level that it is difficult to conceive of what we would recognize as a functioning society without these luxuries. Equally, it makes it difficult to imagine ever losing our ability to exercise such fine control over our immediate microbial environment. Simply put, there are few modern technologies that are as profoundly fundamental to the proper functioning of our society as antimicrobial control.

However, the profligate administration of antibiotics since the mid 20th century has now led to widespread antimicrobial resistance (AMR), threatening to return medicine to the “dark ages” before widespread availability of microbial control [1]. With the World Health Organization (WHO) announcement in 2014 that AMR was no longer a looming threat but a contemporary crisis [2], the problem of antibiotic resistance is proving increasingly salient [3].

At the same time, in a global context where common pathogenic bacterial strains are rapidly gaining new resistance mechanisms, the pharmaceutical sector is largely withdrawing from the antibiotic discovery field, which has led to a failure to discover any new classes of antimicrobial agents in over three decades [4], [5].

1.1 Bacteriophage therapy

A growing appreciation for the importance of antibiotic stewardship and the urgency of identifying novel therapies has led to renewed interest in bacteriophage therapy as a plausible replacement for antibiotics [6]. Bacteriophages, may represent an essential component of a new treatment paradigm, one in which antibiotics are either supplanted entirely, or used in tandem with bacteriophage preparations. Such treatment is known as “bacteriophage therapy”.

Bacteriophages – also known as ‘phages’ – are obligate intracellular parasitic viruses that replicate only in their host bacterium [7], [8]. Crucially for the present work, phages recognize and bind to their host bacterium surface *via* receptor-binding domains (RBDs) – epitope-recognizing regions on the phage capsid.

Phage structure exhibits large variation which falls within a few stereotyped forms (**Erreur ! Source du renvoi introuvable.Erreur ! Source du renvoi introuvable.**). Phage morphology can be grouped into long contractile-tailed (*Myoviridae*), long non-contractile-tailed (*Siphoviridae*), short-tailed (*Podoviridae*), and filamentous (*Inoviridae*) [9]. Phages are also described in terms of their replication cycle. *Lytic phages* terminate their replicative cycle with the

biochemical lysis of their host, rupturing the cell membrane and releasing up to several hundred progeny virions in one burst. In contrast, *lysogenizing* phages incorporate their genetic code into that of the bacterial cell and may lay dormant before shifting to a lytic cycle, or may instead continually produce a smaller number of phages which are shed from the host on a continuous basis [10]. Lytic phages are preferred for the purposes of phage therapy since they are immediately lethal to their host bacteria and are less likely to confer virulence factors to the latter via horizontal gene transfer.

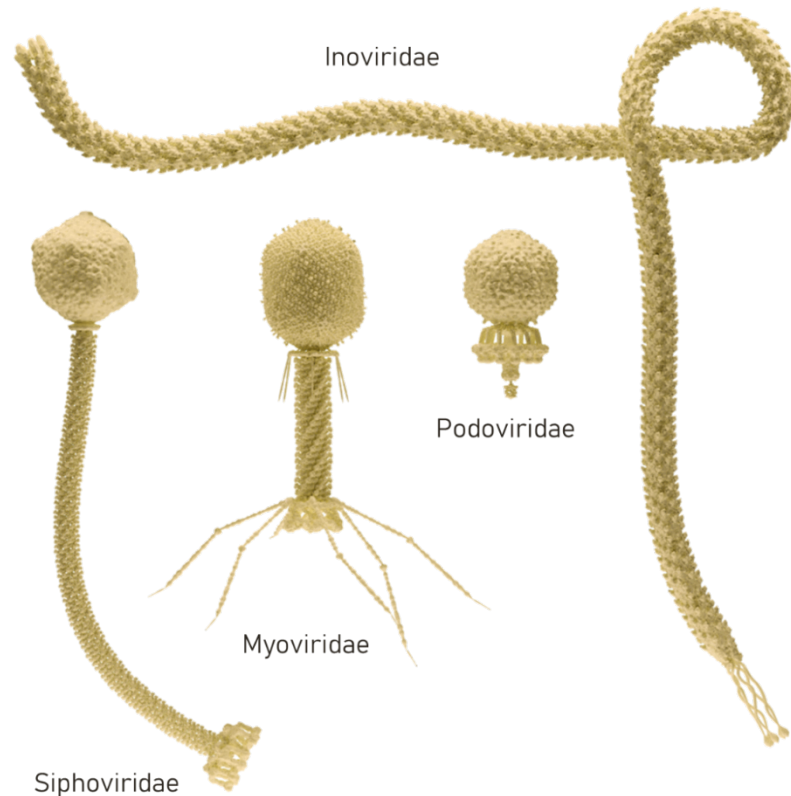


Figure 1. Illustrations of the bacteriophage morphologies that appear most often in the phage-functionalization literature. The Inoviridae family includes phages such as fd and M13. The Myoviridae family includes the well-known T4 coliphage. Meanwhile, the Podoviridae family includes P22.

The independent discovery of phages by microbiologists Frederick Twort and Felix d’Herelle in 1915 and 1917, respectively [11], eventually led to their widespread use in the Soviet Union for the treatment of routine bacterial infections, beginning in 1938 the soviet military campaign in Finland and later in World War II [12]. Meanwhile in the West, the discovery by Alexander Fleming in 1928 of penicillin – a broad spectrum antibiotic – led to a paradigm shift in medicine that relied heavily on the widespread administration of what was seen at the time as the “magic bullet” that antibiotics represented.

The geopolitical paranoia of the Cold War and a lack of scientific rigor in reporting of early soviet phage therapy studies resulted in a progressive dismissal of phage therapy in Western medicine [13]. In the 1970s, up to 70 patients per year underwent phage therapy to treat bone and joint infections (BJI) in Croix Rousse Hospital, Lyon[14]. However, non soviet-aligned states instead pursued a policy of unfettered use of antibiotics [15]. Now, after a 60-year hiatus in western medicine, treatment of antimicrobial infections is receiving renewed attention.

In order to facilitate such an epochal transition to phage therapy, we must develop tools that are analogous to those already used for antibiotic susceptibility testing (AST); a term that refers to a range of methods used to reveal the set of antimicrobials that are effective against a given bacterial strain. In a clinical context, a classic AST method is the *Kirby-*

Bauer or *disk diffusion test*, used since the 1960s.[16] In the disk diffusion test, a small absorbent disk is impregnated with an antimicrobial agent of interest and the disk is then placed on a recently inoculated bacterial lawn and incubated on a standard agar plate. The antimicrobial agent will diffuse out of the disk into the surrounding agar, thus inhibiting the proliferation of bacteria in a visible region known as the *zone of inhibition* (**Erreur ! Source du renvoi introuvable.**). The antimicrobials that produce the largest zone of inhibition are revealed as the most effective against the inoculated bacterial strain and are thus good candidates for administration to the patient.

Phage susceptibility testing (PST) proceeds in a similar way, typically relying on spot testing or culture lysis followed by the more precise *agar overlay* method.[17] In spot testing, a solution suspected to contain effective phages is placed in small drops over a bacterial lawn of the target host bacterial strain and incubated. A phage's ability to lyse the challenge strain and replicate will manifest as visible "lysis plaques" in the surface of the agar, where the proliferating phage progeny lyse bacteria, inhibiting their growth (**Erreur ! Source du renvoi introuvable.**). The surrounding bacterial lawn becomes opaque due to bacterial growth unhindered by phage replication.

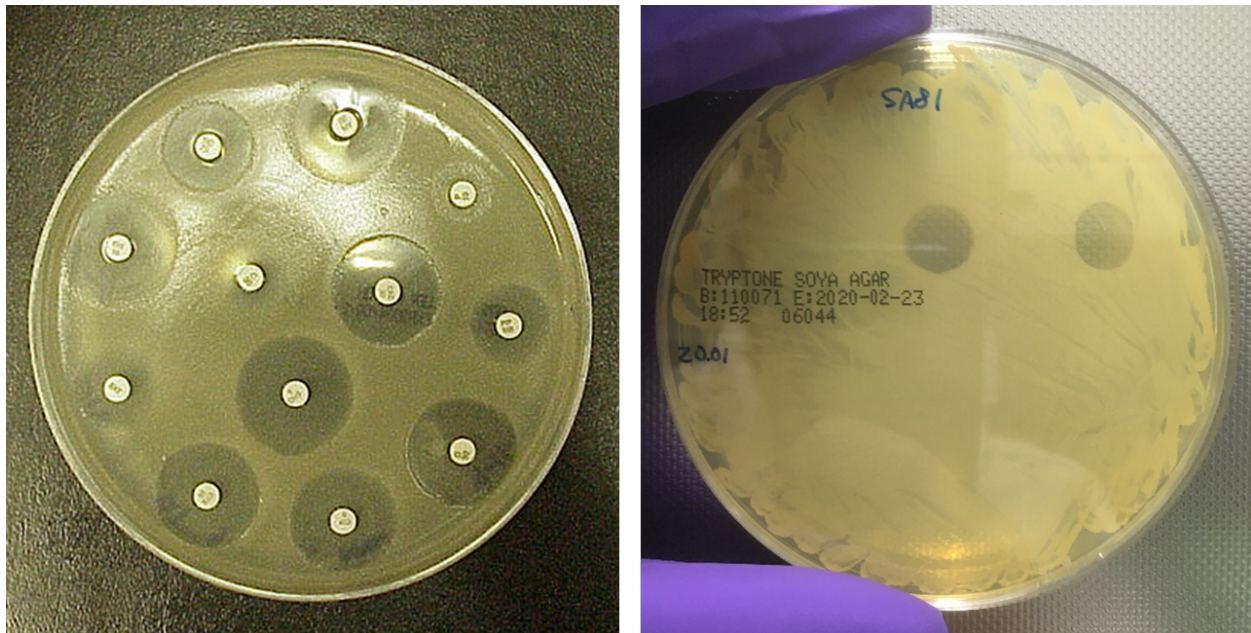


Figure 2. At left, typical disk diffusion test by which a bacterial strain is tested for its susceptibility to multiple antibiotic-impregnated wafers. At right, drops of bacteriophages 44AHJD and K were incubated with *Staphylococcus aureus*, lysing the cells and producing regions of lysis.

Although accurate, a drawback of this form of PST stems from the very large number of candidate phages that must be screened compared to the relatively small number of available antimicrobial agents. It quickly becomes impractical to test a bacterial strain for susceptibility to dozens or even hundreds of candidate bacteriophages. PST methods must be developed that are capable of simultaneously screening a large number of candidate phages rapidly and in parallel.

The current work proposes an affinity biosensor, where the measurand is the binding affinity between a challenge bacterial strain (suspended in a mobile phase – a microfluidic flow) and an array of many candidate phages (immobilized on a stationary phase – an SPR prism).

Crucially for the present work, phages recognize and bind to their host bacterium surface *via* receptor-binding domains (RBDs) – epitope-recognizing regions on the phage capsid. The ability of phages to specifically recognize and bind to their host bacteria allows their use as immobilized probes for those bacteria[18]–[24]. We conjecture that the differential SPR signal between regions functionalized with different candidate phages, in response to the presence of a challenge strain of bacteria, will allow us to rapidly identify phages that are effective at lysing that challenge strain. Thus the 'phagogram' is to phage therapy what antibiotic-susceptibility testing is to classical antibiotic therapy. To our knowledge no example yet exists in the literature for SPR-based phage susceptibility screening.

1.2 The SPR phenomenon

When light travels from a medium with a high refractive index (RI) into a medium with a lower one, it can undergo total internal reflection (TIR) provided that the incident angle is larger than the critical angle[25]. In a TIR regime, when incident on the interface between these two media, the photon generates an evanescent field which penetrates some distance into the lower RI medium. This evanescent field strength is maximal at the interface between the two materials but decays exponentially and is negligible further than a few hundred nanometers into the lower-RI medium. This distance varies as a function of the incident light wavelength and is known as the ‘penetration depth’ of the field[25]. Changes in the RI within the penetration depth manifest as small changes in the amplitude of reflected light.

Surface plasmon resonance (SPR) improves this sensitivity to RI changes. While SPR can be achieved with several different configurations (e.g. waveguide, prism, and grating coupling), here we will focus briefly on the Kretschmann configuration of prism coupling since this is the technique exploited in the present work. A thin metallic layer (typically gold) is deposited on the surface of a high-RI glass prism and exposed to a dielectric (e.g. an aqueous solution). Charge-density oscillations known as surface plasmon polaritons (SPPs) are naturally present at the metal-dielectric interface[25], [26]. Photons incident from the metal side of the interface, when exhibiting a specific combination of wavelength and incident angle, can generate a TIR evanescent field which can excite an SPP evanescent field which in turn couples to and enhances the TIR evanescent field. This coupling mechanism is highly sensitive to fluctuations in the RI within the penetration depth of the evanescent field into the dielectric.

Molecular interactions at the surface – for example between an immobilized stationary phase and an analyte suspended in the mobile phase – can lead to mass uptake which alters the local refractive index within the vicinity of the surface. This alters the resonance conditions between incident photons from the metal side and the SPPs at the interface, which in turn leads to an angular shift in the reflectance from that region. Functionalization of different regions of the surface with different molecular probes leads to divergent molecular interactions and hence yields a differential signal, the evolution of which give information on the interaction kinetics of each probe with the analyte.[25]

Two key strengths of SPR are the high sensitivity to RI changes near the surface, and the ability to simultaneously monitor the interaction kinetics with an array of different immobilized probes. In this work we hope to leverage both by immobilizing an array of many candidate phages on the SPR prism surface, and to probe their interactions with a challenge strain of bacteria, which will manifest as a detectable SPR shift.

1.3 *Pseudomonas putida* and bacteriophage gh-1 as a model system

Bacteriophage gh-1 (ATCC 12633-B1) is capable of infecting and replicating inside susceptible strains of *Pseudomonas putida*[27], an gram-negative soil bacterium. The motivation for choosing gh-1 and *P. putida* as a model system is three-fold:

- Over 95% of described phages are tailed[28]. Since gh-1 represents a typical *podovirus* morphology, it is reasonable to expect that any techniques developed for processing of gh-1 should be extensible to other commonly used phages.
- Short-tailed phages such as gh-1 are more efficient for bacterial capture, compared to those conjugated to filamentous or long-tailed phages.[29]
- Bacteriophage gh-1 is a lytic phage, as would be any candidate phages used in phage therapy.

2. MATERIALS & METHODS

2.1 Tangential Flow Filtration

Tangential flow filtration (TFF) is carried out using the Pall Minimate™ Tangential Flow Filtration system, using a 500 kD cartridge. Phage lysate is diluted from 40mL to 500mL, concentrated to 10mL, diluted to 500mL again, then finally concentrated to 40mL. The remaining retentate is centrifuged 5000g 10 min 4C, to rid the retentate of any large contaminants from the minimate circuit itself. Further concentration from 40mL to ~1mL is carried out using a 30 kD Vivaspin 20 Ultrafiltration unit.

2.2 Nanoparticle Tracking Analysis

Nanoparticle tracking analysis was carried out at the Institut de Biologie Structural (IBS, Grenoble) on a Nanosight NS300 (Malvern) with camera level 16, detection threshold 10.

2.3 Transmission Electron Microscopy

Transmission electron microscopy (TEM) was carried out at IBS Grenoble according to the negative stain-mica-carbon flotation technique. Samples were adsorbed to the clean side of a carbon film on mica, stained with uranyl acetate (AcUr) $\text{UO}_2(\text{CH}_3\text{COO})_2 \cdot 2\text{H}_2\text{O}$ at 2% in distilled water (pH 4.2-4.5), and transferred to a 400-mesh copper grid. The images were taken under low dose conditions ($<10 \text{ e}^-/\text{\AA}^2$) with defocus values between 1.2 and 2.5 μm on a Tecnai 12 LaB6 electron microscope at 120 kV accelerating voltage using a Camera Gatan Orius 1000 CCD.

2.4 Scanning Electron Microscopy

A thin ~4nm layer of carbon was deposited on phage-functionalized gold substrates using a Safematic CCU-010 HV compact coating unit, at 3×10^{-5} mBar. SEM observations were made *via* secondary electron emission on a Zeiss Ultra 55A, with 2kV acceleration voltage.

2.5 Surface Plasmon Resonance

Surface plasmon resonance measurements are carried out using a custom SPR setup consisting of a SPRi-Biochip prism (Horiba) illuminated with an 880nm light emitting diode and monitored *via* a camera. Challenge strains are introduced to the prism using a $1 \mu\text{L/s}$ flow of PBS (as carrier fluid) through a 2mL an injection loop into a 70 μm internal-height microfluidic chamber above the prism surface.

3. RESULTS

3.1 Nanoparticle Tracking Analysis

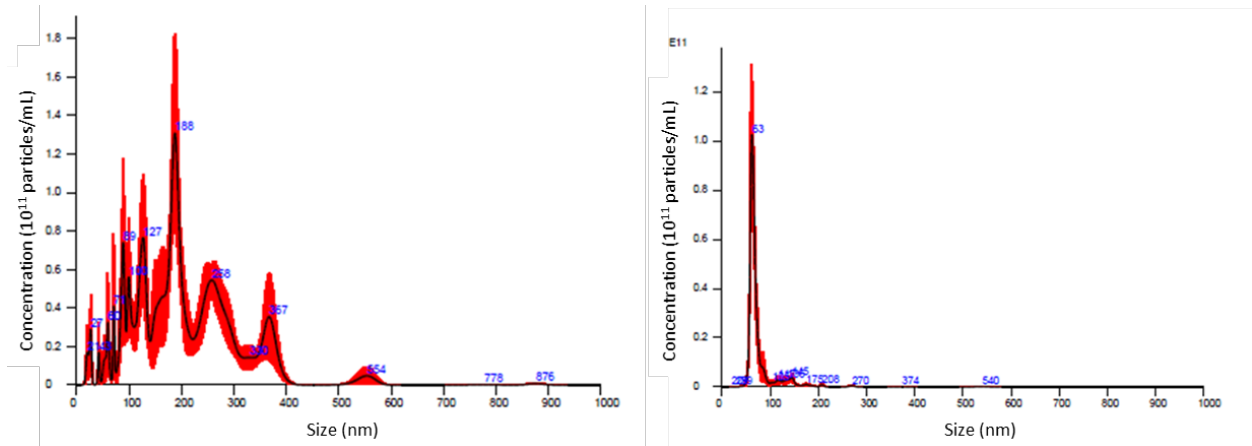


Figure 3. At left, nanoparticle tracking analysis (NTA) of a minimally purified bacteriophage gh-1 suspension: centrifugation at 5000g followed by direct filtration through a 0.2 μm -pore size syringe filter. The suspension shows cellular debris across a large range of length scales, making it unsuitable for immobilization chemistry. At right, NTA results for bacteriophage gh-1 suspension after purification by tangential flow filtration (TFF) and further concentration using a centrifugal concentrator. There is a clearly defined peak at 63nm, which we attribute to the presence of bacteriophage gh-1.

NTA results for our purified phage suspensions exhibit a pronounced peak at 63nm, which is consistent with the hydrodynamic diameter of bacteriophage gh-1[27]. Meanwhile, minimally processed phage suspensions are revealed by NTA to harbor a large range of contaminants other than bacteriophage. These results are complemented by TEM analysis of the same solutions (**Erreur ! Source du renvoi introuvable.**). Although some material other than phage gh-1 is visible in TFF-purified suspensions, we can see in a qualitative way that they represent a marked improvement compared to minimally purified suspensions.

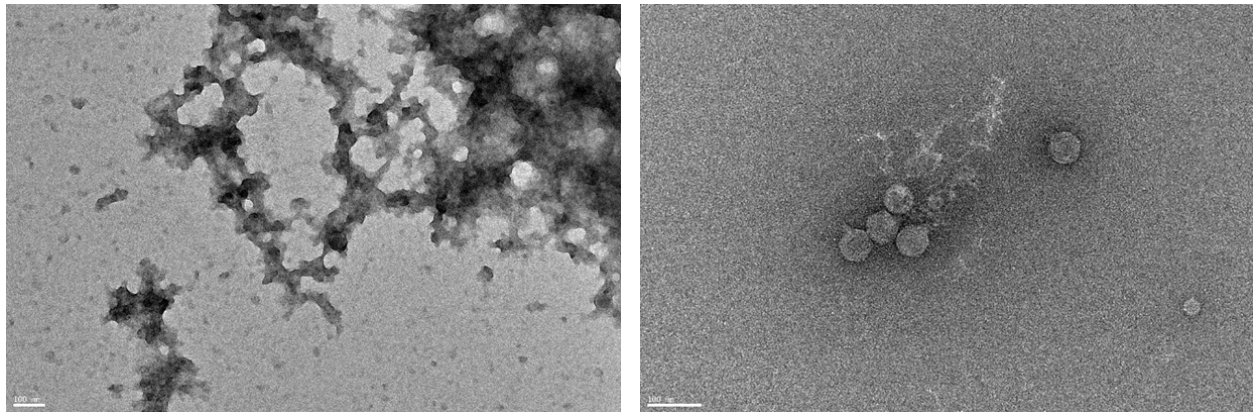


Figure 4. TEM imagery of minimally purified phage suspensions (left) and one purified by tangential flow filtration (TFF)

3.2 Scanning Electron Microscopy

Figure 5. SEM imagery of a typical prism surface, in this case functionalized with bacteriophage gh-1 (left), control lysate of *P. putida* (centre), and 154mM NaCl (right) using electropolymerisation of pyrrole.

SEM analysis appears to show the presence of small spherical 50-100nm clusters after surface functionalization (**Erreur ! Source du renvoi introuvable.**), which supports the assertion that phages have been immobilized on the surface. However, this could equally be cellular debris due to bacterial lysis rather than phage particles. For this reason, a control suspension was produced by mechanically lysing a liquid bacterial culture using high-intensity ultrasound, and then purifying the suspension as if it contained phages. We conjecture that this ‘control lysate’ should contain the same interferents and debris that would survive the purification process but without phages present. Inclusion of this control lysate as one of the immobilized species allows us to confirm that any specific response is due to the phages themselves, and no other component of the phage lysate. Indeed, SEM analysis shows that less material is deposited on regions ‘functionalized’ both with the control lysate and with a control solution of 154mM NaCl.

3.3 Surface plasmon resonance

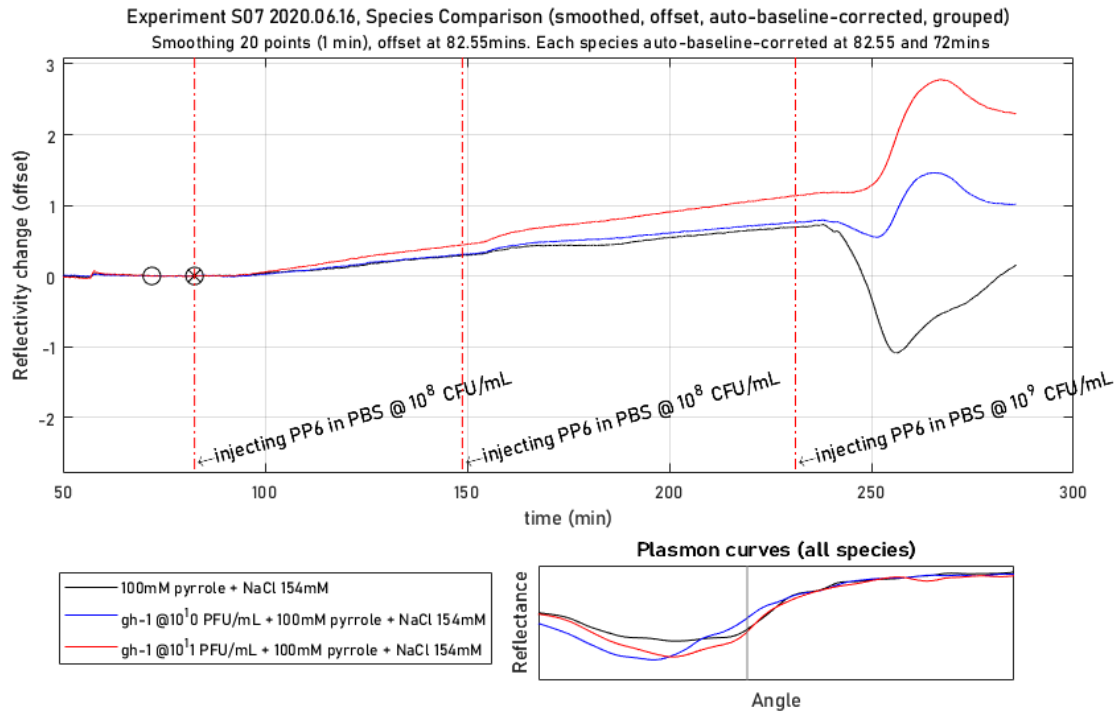


Figure 6. Surface plasmon resonance (SPR) shifts of regions functionalized with various solutions, grouped into 3 different species based on the immobilization solution phage content. Pyrrole concentrations quoted in the legend refer to pyrrole monomer concentrations in solutions used for electropolymerisation of pyrrole on the prism surface, a method that was investigated for the entrapment and immobilization of bacteriophage particles.

Figure 6 shows processed SPR data from a typical SPR experiment wherein gh-1 were immobilized on the surface of an SPR prism, using immobilization solutions of concentrations of 10^{10} and 10^{11} phage/mL, and then subjected to a flow of their host bacterium *P. putida* suspended in PBS. To provide an easier visualization of the response of each cohort, SPR traces have been offset at $t=82.55$ minutes (marked with a cross), and each trace has been baseline corrected according to their evolution at $t=72$ and 82.55 mins (marked with circles). The red trace shows a commensurately elevated SPR response of regions functionalized with the highest phage concentration, especially following the introduction of *P. putida* at 10^9 cells/mL. Red and yellow traces show the response of regions functionalized with a solution with 10x lower phage concentration and exhibit a commensurately smaller SPR response to each injection. However, the response of the control species, which exhibits a marked reduction in reflection, is not expected. We would expect the blank to remain relatively stable in response to the introduction of bacteria.

While such results are somewhat encouraging, further work is needed to find the optimal immobilization conditions to achieve the best SPR response.

4. CONCLUSIONS & OUTLOOK

The project is ongoing and will focus on optimization of the immobilization strategy in order to achieve the strongest specific phage-host interaction and hence the strongest possible SPR response. After an extensive literature review, several potential avenues for improvement have been identified. These include:

Physisorptive immobilization, wherein the phages are simply incubated with a plasma-cleaned gold substrate with no conjugation to the surface[30].

Self-assembled monolayers of various alkanethiols, notably 11-MUA[31], 3-MPA[32], and DTSP[33].

Application of an electric field during functionalization has been demonstrated to yield an improvement in bacterial capture, due to orientation of phage tail fibers (and hence their receptor-binding domains) towards the solution[34].

SPR measurements will be correlated with defocalized microscopy in parallel, in order to provide a visual confirmation of cell attachment and lysis on the prism surface. This is possible since gold-coated glass slides are both compatible with defocalized microscopy and can be phage-functionalized using the same chemistry as were the SPR prisms.

5. ACKNOWLEDGMENTS

This work has been partially supported by Labex Arcane and CBH-EUR-GS (ANR-17-EURE-0003), with experiments carried out at SyMMES and CEA, Grenoble, France.

Among others, many thanks to my PhD co-supervisors Yoann Roupioz (SyMMES, Grenoble) and Pierre Marcoux (LSIV, CEA Grenoble); Christine Chatellard (Institut de Biologie Structurale, Grenoble), for her assistance with Nanoparticle Tracking Analysis; Raphaël Mathey (SyMMES, CEA, Grenoble), for assistance with bacterial culture and immobilization chemistry; Prisca Perlemoine (LSIV, CEA, Grenoble), for assistance with phage amplification techniques; Ondrej Mandula (LSIV, CEA, Grenoble), for the development and loan of a defocalized microscope; Grégory Resch (UNIL, Lausanne), for advice related to culture of gh-1 phages.

Phage gh-1 (ATCC 12633-B1) provided by the Félix d'Hérelle Reference Center for Bacterial Viruses, Université de Laval, QC, Canada.

This work used the EM facilities at the Grenoble Instruct-ERIC Center (ISBG; UMS 3518 CNRS CEA-UGA-EMBL) with support from the French Infrastructure for Integrated Structural Biology (FRISBI; ANR-10-INSB-05-02) and the Grenoble Alliance for Integrated Structural Cell Biology (GRAL; ANR-10-LABX-49-01) within the Grenoble Partnership for Structural The IBS Electron Microscope facility is supported by the Auvergne Rhône-Alpes Region, the Fonds Feder, the Fondation pour la Recherche Médicale and GIS-IBiSA.

All image credits are to the author unless otherwise stated.

References for protein structures used in illustrations:

Cryo-electron microscopy structure of the hexagonal pre-attachment T4 baseplate-tail tube complex

PDB ID: 5IV5

Taylor, N.M. et al. (2016) Structure of the T4 baseplate and its function in triggering sheath contraction. *Nature* 533: 346-352

CryoEM single particle reconstruction of prolate head of bacteriophage T4

EMD ID: 6323

Sun, L. et al. (2015) Cryo-EM structure of the bacteriophage T4 portal protein assembly at near-atomic resolution in *Nat Commun* 6, 7548

Fitting of gp18M crystal structure into 3D cryo-EM reconstruction of bacteriophage T4 extended tail PDB ID: 3FOH

Aksyuk et al. (2009) The tail sheath structure of bacteriophage T4: a molecular machine for infecting bacteria in *EMBO J* 28(7):821-9

Structure of native bacteriophage P68

PDB ID: 6Q3G

Hrebík et al. (2019) Structure and genome ejection mechanism of *Staphylococcus aureus* phage P68 in *Sci Adv.* 16;5(10):eaaw7414

Structure of the bacteriophage C1 tail knob protein, gp12

PDB ID: 4EO2

Aksyuk et al. (2012) Structural investigations of a Podoviridae streptococcus phage C1, implications for the mechanism of viral entry in *Proc.Natl.Acad.Sci.USA* 109: 14001-14006

Localized reconstruction of tail-spike of bacteriophage P68

PDBJ ID: EMD-4450

Hrebík et al. (2019) Structure and genome ejection mechanism of *Staphylococcus aureus* phage P68 in *Sci Adv.* 16;5(10):eaaw7414

Capsid model of M13 bacteriophage virus from Magic-angle spinning NMR and Rosetta modeling

PDB ID: 2mjz

Morag, O. et al. (2015) The NMR-Rosetta capsid model of M13 bacteriophage reveals a quadrupled hydrophobic packing epitope in *Proc Natl Acad Sci USA* **112**: 971-976

Crystal structure of Bovine Serum Albumin

PDB ID: 3v03

Majorek et al. (2012) Structural and immunologic characterization of bovine, horse, and rabbit serum albumins in *Mol.Immunol.* 52: 174-182

REFERENCES

- [1] D. Elhani, "L'émergence de la résistance aux antibiotiques annonce-t-elle le retour des âges sombres?," *Ann. Biol. Clin. (Paris)*, vol. 69, no. 6, pp. 637–646, 2011, doi: 10.1684/abc.2011.0632.
- [2] "Antimicrobial Resistance Global Report on Surveillance," 2014.
- [3] Jim O'Neill, "Antimicrobial Resistance : Tackling a crisis for the health and wealth of nations," *Rev. Antimicrob. Resist.*, no. December, pp. 1–16, 2014, doi: 10.1038/510015a.
- [4] S. J. Projan, "Why is big Pharma getting out of antibacterial drug discovery?," *Curr. Opin. Microbiol.*, vol. 6, no. 5, pp. 427–430, 2003, doi: 10.1016/j.mib.2003.08.003.
- [5] C. E. Broughton, H. A. Van Den Berg, A. M. Wemyss, D. I. Roper, and A. Rodger, "Beyond the discovery void: New targets for antibacterial compounds," *Sci. Prog.*, vol. 99, no. 2, pp. 153–182, 2016, doi: 10.3184/003685016X14616130512308.
- [6] A. Kakasis and G. Panitsa, "Bacteriophage therapy as an alternative treatment for human infections. A comprehensive review," *Int. J. Antimicrob. Agents*, vol. 53, no. 1, pp. 16–21, 2019, doi: 10.1016/j.ijantimicag.2018.09.004.
- [7] K. E. Wommack and R. R. Colwell, "Virioplankton: viruses in aquatic ecosystems," *Microbiol. Mol. Biol. Rev.*,

- vol. 64, no. 1, pp. 69–114, Mar. 2000, doi: 10.1128/mmbr.64.1.69-114.2000.
- [8] S. Chibani-chennoufi, A. Bruttin, H. Brüssow, M. Dillmann, and H. Bru, “Phage-Host Interaction : An Ecological Perspective,” *J. Bacteriol.*, vol. 186, no. 12, pp. 3677–3686, 2004, doi: 10.1128/JB.186.12.3677.
- [9] J. M. W. Prescott, L. Sherwood, C. J. Woolverton, and L. M., “Chapter 17 - The Viruses: Viruses of Bacteria and Archaea,” in *Microbiology*, 7th ed., McGraw-Hill, Ed. 2008, pp. 427–446.
- [10] Richard Calendar, *The Bacteriophages*, 2nd ed. Oxford University Press, 2006.
- [11] D. H. Duckworth, “Who Discovered Bacteriophage?,” *Bacteriol. Rev.*, vol. 40, no. 4, pp. 793–802, 1976.
- [12] D. Myelnikov, “An Alternative Cure: The Adoption and Survival of Bacteriophage Therapy in the USSR, 1922-1955,” *J. Hist. Med. Allied Sci.*, vol. 73, no. 4, pp. 385–411, 2018, doi: 10.1093/jhmas/jry024.
- [13] W. C. Summers, “Bacteriophage Therapy,” *Annu. Rev. Microbiol.*, no. 55, pp. 437–51, 2001.
- [14] T. Ferry *et al.*, “Phage therapy in bone and joint infection: history, scientific basis, feasibility and perspectives in France.,” *Virologie*, vol. 24, no. 1, pp. 49–56, Feb. 2020, doi: 10.1684/vir.2020.0808.
- [15] S. B. Levy and M. Bonnie, “Antibacterial resistance worldwide: Causes, challenges and responses,” *Nat. Med.*, vol. 10, no. 12S, pp. S122–S129, 2004, doi: 10.1038/nm1145.
- [16] A. W. BAUER, W. M. . M. . KIRBY, J. . C. . SHERRIS, and M. TURCK, “Antibiotic Susceptibility Testing by a Standardized Single Disk Method,” *Am. J. Clin. Pathol.*, vol. 45, no. 4, pp. 493–496, 1966.
- [17] P. Hyman, “Phages for Phage Therapy: Isolation, Characterization, and Host Range Breadth,” *Pharmaceuticals*, vol. 12, no. 1, p. 35, 2019, doi: 10.3390/ph12010035.
- [18] R. S. Lakshmanan, R. Guntupalli, J. Hu, V. A. Petrenko, J. M. Barbaree, and B. A. Chin, “Detection of Salmonella typhimurium in fat free milk using a phage immobilized magnetoelastic sensor,” *Sensors Actuators, B Chem.*, vol. 126, no. 2, pp. 544–550, 2007, doi: 10.1016/j.snb.2007.04.003.
- [19] I. H. Chen, S. Horikawa, K. Bryant, R. Riggs, B. A. Chin, and J. M. Barbaree, “Bacterial assessment of phage magnetoelastic sensors for Salmonella enterica Typhimurium detection in chicken meat,” *Food Control*, vol. 71, pp. 273–278, 2017, doi: 10.1016/j.foodcont.2016.07.003.
- [20] E. V. Olsen, I. B. Sorokulova, V. A. Petrenko, I. H. Chen, J. M. Barbaree, and V. J. Vodyanoy, “Affinity-selected filamentous bacteriophage as a probe for acoustic wave biodetectors of Salmonella typhimurium,” *Biosens. Bioelectron.*, vol. 21, no. 8, pp. 1434–1442, 2006, doi: 10.1016/j.bios.2005.06.004.
- [21] R. Guntupalli *et al.*, “Detection and identification of methicillin resistant and sensitive strains of Staphylococcus aureus using tandem measurements,” *J. Microbiol. Methods*, vol. 90, no. 3, pp. 182–191, 2012, doi: 10.1016/j.mimet.2012.05.003.
- [22] F. He, M. Xiang, and X. Mi, “A New Bacteriophage-Modified Piezoelectric Sensor for Rapid and Specific detection of Mycobacterium,” *Anal. Lett.*, vol. 45, no. 10, pp. 1242–1253, Jul. 2012, doi: 10.1080/00032719.2012.673106.
- [23] R. S. Burlage and J. Tillmann, “Biosensors of bacterial cells,” *J. Microbiol. Methods*, vol. 138, pp. 2–11, 2017, doi: 10.1016/j.mimet.2016.12.023.
- [24] S. Niyomdecha *et al.*, “Phage-based capacitive biosensor for Salmonella detection,” *Talanta*, vol. 188, no. April, pp. 658–664, 2018, doi: 10.1016/j.talanta.2018.06.033.
- [25] R. B. M. Schasfoort, *Handbook of Surface Plasmon Resonance*, 2nd ed. Royal Society of Chemistry, 2017.
- [26] J. Homola, *Surface Plasmon Resonance Based Sensors (Springer Series on Chemical Sensors and Biosensors, Volume 4)*. .
- [27] L. F. Lee and J. A. Boezi, “Characterization of bacteriophage gh-1 for Pseudomonas putida.,” *J. Bacteriol.*, vol. 92, no. 6, pp. 1821–1827, 1966.
- [28] H. W. Ackermann, “Bacteriophage observations and evolution,” *Res. Microbiol.*, vol. 154, no. 4, pp. 245–251, 2003, doi: 10.1016/S0923-2508(03)00067-6.
- [29] Z. Hosseinidoust, T. G. M. Van De Ven, and N. Tufenkji, “Bacterial capture efficiency and antimicrobial activity of phage-functionalized model surfaces,” *Langmuir*, vol. 27, no. 9, pp. 5472–5480, 2011, doi: 10.1021/la200102z.
- [30] S. Balasubramanian, I. B. Sorokulova, V. J. Vodyanoy, and A. L. Simonian, “Lytic phage as a specific and selective probe for detection of Staphylococcus aureus — A surface plasmon resonance spectroscopic study,” *Biosens. Bioelectron.*, vol. 22, no. 6, pp. 948–955, 2007, doi: 10.1016/j.bios.2006.04.003.
- [31] N. Tawil, E. Sacher, R. Mandeville, and M. Meunier, “Surface plasmon resonance detection of E. coli and methicillin-resistant S. aureus using bacteriophages,” *Biosens. Bioelectron.*, vol. 37, no. 1, pp. 24–29, 2012, doi: 10.1016/j.bios.2012.04.048.
- [32] L. Han, H. Xia, L. Yin, V. A. Petrenko, and A. Liu, “Selected landscape phage probe as selective recognition

- interface for sensitive total prostate-specific antigen immunosensor,” *Biosens. Bioelectron.*, vol. 106, no. October 2017, pp. 1–6, 2018, doi: 10.1016/j.bios.2018.01.046.
- [33] S. K. Arya, A. Singh, R. Naidoo, P. Wu, M. T. McDermott, and S. Evoy, “Chemically immobilized T4-bacteriophage for specific *Escherichia coli* detection using surface plasmon resonance,” *Analyst*, vol. 136, no. 3, pp. 486–492, 2011, doi: 10.1039/c0an00697a.
- [34] Á. Richter *et al.*, “Ordering of bacteriophages in the electric field: Application for bacteria detection,” *Sensors Actuators B Chem.*, vol. 224, pp. 233–240, 2016, doi: 10.1016/j.snb.2015.09.042.